Spatial Distribution of Magnetic Field under Spherical Shell Plasma

Xinhua Song[1], Honghao Yan[1, *], Zhengzheng Ma[2], Yang Wang[1], and Bing Xu[2]

Abstract—Magnetic field intensity is modeled using Laplacian equations to study the spatial distribution of magnetic field under spherical shell plasma. The influences of different internal and external radii are also considered. In addition, the magnetic field calculation of plasma space is analyzed. The main conclusions are as follows. The external uniform magnetic field H_0 is the scalar magnetic bit, and the magnetic charge of the shell of the plasma is equivalent to that of a magnetic dipole. The magnetic field in the spherical shell is a superposition of a uniform field and a magnetic dipole field. The uniform field is composed of an externally applied uniform field H_0 and a uniform field generated by the magnetic charge on the outer surface of the ball. The magnetic dipole field is generated by the magnetic charge on the inner surface of the shell, and the inside of the shell is a uniform magnetic field. When μ_2/μ_1 is high and a/b is low, the ratio of the magnetic field strength H_3 (the region is $r < a$) to the magnetic field strength H_0 (the region is $r > b$) is low. By contrast, when μ_2/μ_1 and a/b are high, the ratio of the magnetic field strength H_3 to the magnetic field strength H_0 is high. When the magnetic permeability of the inner object is small and the spherical shell is thick, the produced plasma sheath is thick, and the external magnetic field in the spherical shell is weak. Therefore, when the shielding effect is good, the possibility that the "black barrier" phenomenon will occur is high, and ground radar detection will be difficult.

1. INTRODUCTION

The research scope of plasma includes high- and low-temperature plasma physics, space plasma physics, and dusty plasma physics, along with the applications of plasma in mechanics, chemistry, medicine, spatial communication, and developing energy [1]. The applications of plasma include plasma stealth [2, 3] and "black barrier" technology [4–8], which are current research hotspots. Plasma stealth technology refers to the use of plasma to avoid radar echo, whereas black barrier refers to the communication interruption that occurs when a shuttle reenters the atmosphere. With high-speed movement, the surface of the shuttle is burdened by a certain thickness of plasma layer (i.e., the plasma sheath) for electromagnetic wave reflection, scattering, and absorption. In recent years, many scholars have worked on various aspects of plasma, such as theoretical research, computational simulation, communication experiment, and flight experiment, and have achieved considerable success.

In 1961, Hodara proposed that the attenuation problem of the right circular polarization wave in plasma would be reduced by adding a magnetic field [9]. During the 1960s, Russo and Hughs conducted a transwave experiment on reentry plasma sheath, which proved that external magnetic fields could reduce communication disruption [10]. To verify the effect of a magnetic field on a plasma sheath, NASA conducted two ground experiments and one flight experiment in 1964. In the ground experiment, NASA added 750 Gauss of magnetic induction to the plasma, with a collision frequency of 1 GHz, thickness of 4 cm, and electron density of 3×10^{11} cm^{-3}. The experimental results showed that the attenuation

degree of the signal was reduced from 60 dB to 40 dB without increasing the magnetic field, thereby proving that an applied magnetic field is effective in reducing the attenuation of electromagnetic waves in plasma [11]. In 2008, Keidar et al. studied the influence of plasma on electromagnetic wave attenuation by theoretically examining applied electric and magnetic fields [12]. In 2009, Kim et al. used a 2D magnetic structure based on experimental data to determine if a 2D magnetic field model would be more effective than a 1D magnetic field model [13].

The aforementioned scholars analyzed the "black barrier" phenomenon caused by plasma through theoretical research, computational simulation, and experimental analysis. Solving the "black barrier" phenomenon is highly significant. However, most present studies have focused on 1D and 2D theories and numerical simulations, and research on the magnetic field calculation of the spatial distribution of a plasma ball remains minimal. On the basis of previous studies, the current work focuses on the magnetic field calculation of the spatial distribution of a plasma ball shell.

2. PHYSICAL MODEL

Assume that a uniform external magnetic field H_0 passes through spherical space and surrounds the plasma of an object. Then, the magnetic permeability of the intermediate object is μ_1, and the spatial distribution of plasma permeability is μ_2. The inner and outer radii are a and b, as shown in Fig. 1.
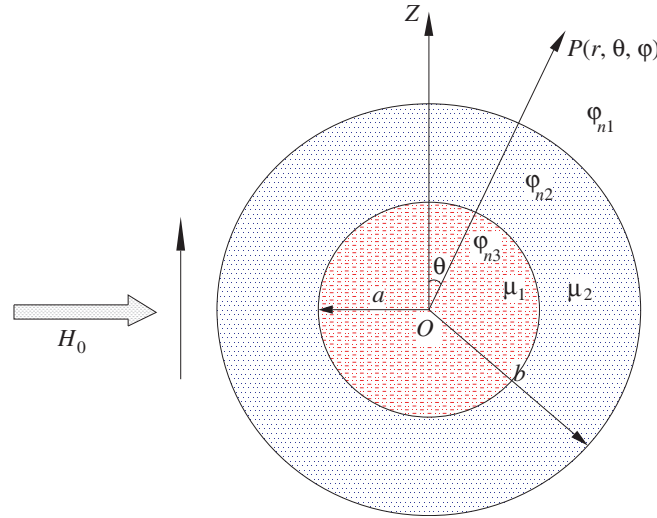

Figure 1. Space distribution model of spherical shells.

The scalar magnetic bits of each district are φ_{n1}, φ_{n2}, and φ_{n3}, all of which satisfy the following Laplacian equations:

$$\begin{cases} \nabla^2 \varphi_{n1} = 0 \, (r > b) \\ \nabla^2 \varphi_{n2} = 0 \, (a < r < b) \\ \nabla^2 \varphi_{n3} = 0 \, (r < a) \end{cases} . \tag{1}$$

Their general solutions are

$$\begin{cases} \varphi_{n1} = \sum_{n=0}^{\infty} \left(A_n r^n + B_n r^{-(n+1)} \right) P_n(\cos\theta) \, (r > b) \\ \varphi_{n2} = \sum_{n=0}^{\infty} \left(C_n r^n + D_n r^{-(n+1)} \right) P_n(\cos\theta) \, (a < r < b) \\ \varphi_{n3} = \sum_{n=0}^{\infty} \left(E_n r^n + F_n r^{-(n+1)} \right) P_n(\cos\theta) \, (r < a) \end{cases} . \tag{2}$$

$P_n(\cos\theta)$ denotes the Legendre polynomials. A_n, B_n, C_n, D_n, E_n, and F_n are the coefficients of the general solutions. When the following boundary conditions are used: $r = 0$, φ_{n3} is limited; $r \to \infty$, $\varphi_{n1} = -H_0 r \cos\theta$; $r = a$, $\varphi_{n3} = \varphi_{n2}$, $\mu_1 \frac{\partial \varphi_{n3}}{\partial r} = \mu_2 \frac{\partial \varphi_{n2}}{\partial r}$; $r = b$, $\varphi_{n1} = \varphi_{n2}$, $\mu_1 \frac{\partial \varphi_{n1}}{\partial r} = \mu_2 \frac{\partial \varphi_{n2}}{\partial r}$.

The coefficients are calculated as follows:

$$
\begin{cases}
A_1 = -H_0 \\[2mm]
B_1 = H_0 \left(\dfrac{\mu_2}{\mu_1} - 1 \right) \left(1 + 2\dfrac{\mu_2}{\mu_1} \right) \left(b^3 - a^3 \right) / K \\[2mm]
C_1 = -3H_0 \left(1 + 2\dfrac{\mu_2}{\mu_1} \right) / K \\[2mm]
D_1 = -2H_0 \left(\dfrac{\mu_2}{\mu_1} - 1 \right) a^3 / K \\[2mm]
E_1 = -9H_0 \dfrac{\mu_2}{\mu_1} / K \\[2mm]
F_1 = 0
\end{cases}
\tag{3}
$$

where $K = (1 + 2\frac{\mu_2}{\mu_1})(2 + \frac{\mu_2}{\mu_1}) - 2(\frac{a}{b})^3(\frac{\mu_2}{\mu_1} - 1)^2$.

When Eq. (3) is substituted into Eq. (2), Eq. (4) can be expressed as follows:

$$
\begin{cases}
\varphi_{n1} = -H_0 r \cos\theta + \dfrac{H_0}{K}\left[2\left(\dfrac{\mu_2}{\mu_1}\right)^2 - \left(\dfrac{\mu_2}{\mu_1}\right) - 1 \right](b^3 - a^3)\dfrac{\cos\theta}{r^2} \; (r > b) \\[3mm]
\varphi_{n2} = -3\dfrac{H_0}{K}\left(1 + 2\dfrac{\mu_2}{\mu_1} \right) r \cos\theta - 3\dfrac{H_0}{K}\left(\dfrac{\mu_2}{\mu_1} - 1 \right) a^3 \dfrac{\cos\theta}{r^2} \; (a < r < b) \\[3mm]
\varphi_{n3} = -9\dfrac{H_0}{K}\dfrac{\mu_2}{\mu_1} r \cos\theta \; (r < a)
\end{cases}
\tag{4}
$$

The magnetic field strength of each region can be obtained from $\vec{H} = -\nabla\varphi_n$.

3. NUMERICAL SIMULATION

3.1. Impacts of Internal and External Radii

Assume that the magnetic field strength H_0 is $10\,\text{A/m}$, $\mu_2 \approx \mu_0$ [14], $\mu_1 \approx 20\mu_0$ [15], where μ_0 is the vacuum permeability. The magnetic distribution diagrams of the magnetic field are calculated as shown in Fig. 2 by changing the kernel radius a and plasma radius b as shown in Table 1.

Table 1. Different a and b parameters.

| Computational Simulation Number	a/m	b/m	a/b
Simulation 1	1	4	1/4
Simulation 2	2	4	2/4
Simulation 3	3	4	3/4
Simulation 4	4	4	4/4

Under the scalar magnetic field of the external uniform magnetic field H_0, the magnetic charge of the plasma shell is equivalent to that of a magnetic dipole. The magnetic field in the plasma shell is the superposition of a uniform field and a magnetic dipole. The uniform field is composed of an externally applied uniform field H_0 and a uniform field generated by the magnetic charge on the outer surface of the ball. The magnetic dipole field is generated by the magnetic charge on the inner surface of the shell. The magnetic field distribution maps of each region under different a/b ratios are obtained by changing the values of a and b, as shown in Fig. 2. The value a/b is asmaller ratio of $H_3(r < a)$ than the field strength $H_0(r > b)$. When a/b is high, H_3/H_0 is also high.
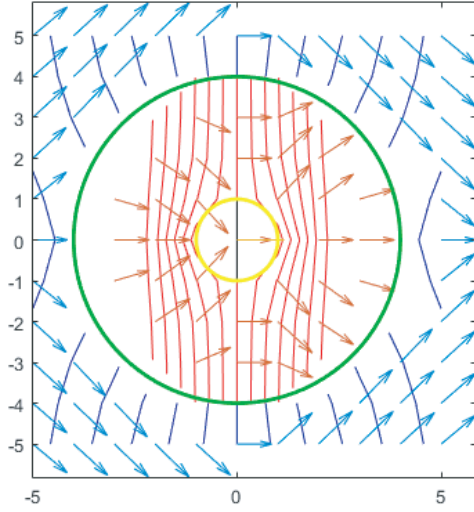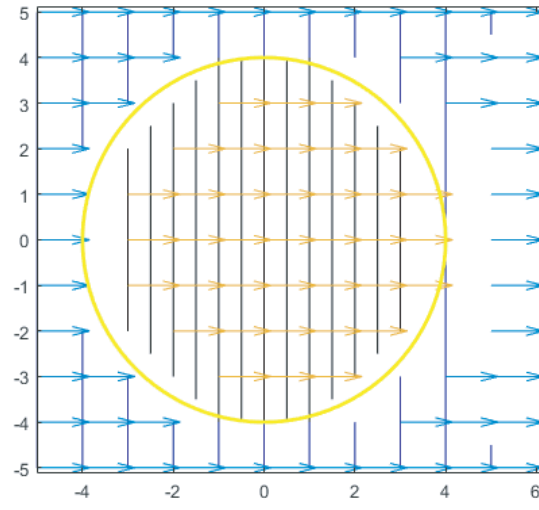
Simulation 1: Magnetic field distribution when a/b = 1/4
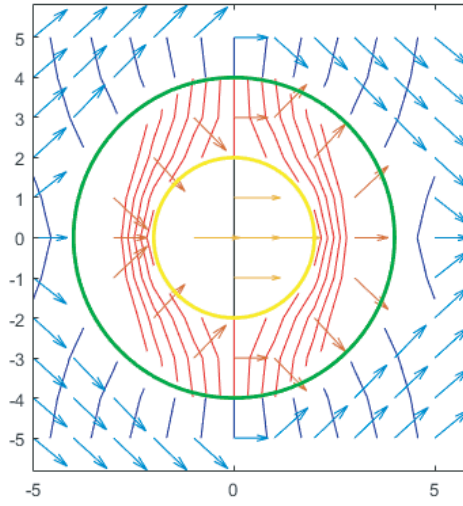
Simulation 2: Magnetic field distribution when a/b = 2/4
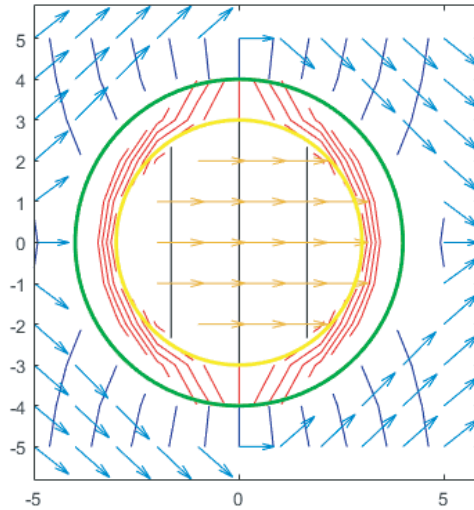
Simulation 3: Magnetic field distribution when a/b = 3/4

Simulation 4: Magnetic field distribution when a/b = 4/4

**Figure 2.** Simulations 1, 2, 3, and 4 that correspond to the magnetic field distribution.

3.2. Influence of Different Permeabilities

When the material of the magnet differs, the corresponding magnetic conductivity also varies. Assume that the magnetic field strength H_0 is $10\,\text{A/m}$. Then, the values of μ_1 are provided in Table 2, and the distributions of magnetic fields are shown in Fig. 3.

The magnetic field on the plasma spherical shell is equivalent to a magnetic dipole in the external magnetic field. It is a superposition of a uniform field with a magnetic dipole. The magnetic dipole field is generated by the magnetic charge on the inner surface of the shell. Different μ_2/μ_1 ratios and the simulation of the magnetic field distribution are obtained as shown in Fig. 3 by changing the internal object material of the plasma spherical shell, i.e., with different magnetic permeabilities, as shown in Table 2. When μ_2/μ_1 is high, the magnetic field strength $H_3(r < a)$ and the magnetic field strength $H_0(r > b)$ are strong. When μ_2/μ_1 is low, the ratio of the magnetic field strength $H_3(r < a)$ to the magnetic field strength $H_0(r > b)$ is high. In other words, the magnetic sphere of the plasma spherical shell is approximately the same as the magnetic permeability of the inner shell, and the magnetic field in the inner space of the spherical shell is relatively strong.

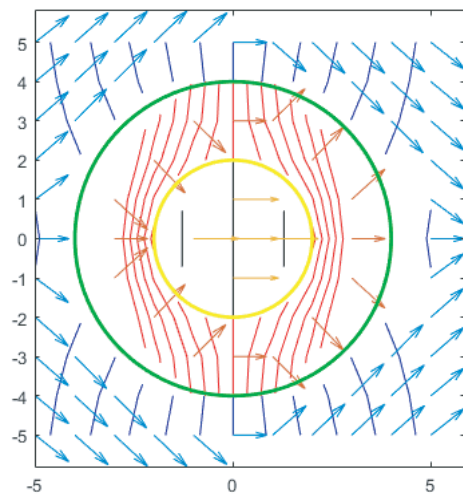**Table 2.** Experimental schemes with different magnetic permeabilities.

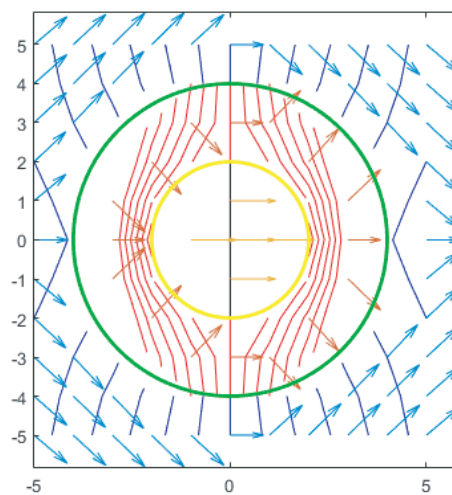| Computational Simulation Number	a/m	b/m	μ_1
Simulation 1	2	4	$0.1\mu_0$
Simulation 2	2	4	μ_0
Simulation 3	2	4	$10\mu_0$
Simulation 4	2	4	$100\mu_0$
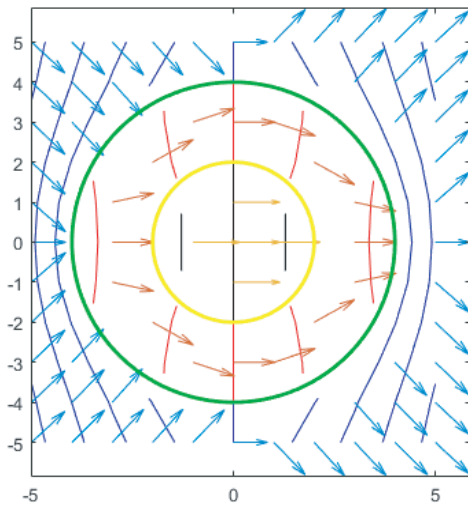
Simulation 1: Magnetic field distribution when $\mu_2/\mu_1 = 10$
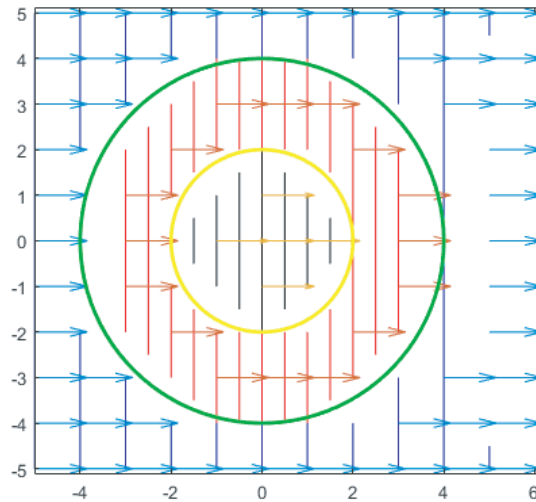
Simulation 2: Magnetic field distribution when $\mu_2/\mu_1 = 1$

Simulation 3: Magnetic field distribution when $\mu_2/\mu_1 = 0.1$

Simulation 4: Magnetic field distribution when $\mu_2/\mu_1 = 0.01$

Figure 3. Simulations 1, 2, 3, and 4 that correspond to the magnetic field distribution.

3.3. Analysis and Discussion

The Scalar magnetic potential φ_{n3} in Eq. (4) indicates that the inside of the spherical shell has a uniform magnetic field, which is expressed as

$$\overrightarrow{H_3} = -\nabla \varphi_{n3} = \frac{9\overrightarrow{H_0}\left(\frac{\mu_2}{\mu_1}\right)}{\left(1 + 2\frac{\mu_2}{\mu_1}\right)\left(2 + \frac{\mu_2}{\mu_1}\right) - 2\left(\frac{a}{b}\right)^3\left(\frac{\mu_2}{\mu_1} - 1\right)^2}.$$

When $\mu_2 \gg \mu_1$, $\overrightarrow{H_3} = \frac{9\overrightarrow{H_0}}{2\frac{\mu_2}{\mu_1}[1-(\frac{a}{b})^3]}$, the permeability ratio of μ_1 and μ_2 and the ratio of the internal and external radii a and b have a corresponding effect on the magnetic field in the inner space of the spherical shell. In other words, when the permeability of the spherical shell is large and the spherical shell is thick, the magnetic field in the inner space of the spherical shell, which provides the best shielding effect, is weak. The limit value of H_3/H_0 is $9/(2\frac{\mu_2}{\mu_1})$. The permeability of the plasma layer outside the object cannot approach 0; hence, achieving complete shielding effect is difficult.

3.4. Calculation Verification

The range of the radar electromagnetic wave is $2 \sim 18$ GHz; therefore, we use 8 GHz to calculate the magnetic field strength in 0.04 T. In 2005, Yang et al. used the calculation method for electromagnetic wave propagation in non-magnetized plasma to obtain the reflection coefficient of an electromagnetic field incident that exhibits vertical magnetism in magnetized plasma [16]. With different electromagnetic wave frequencies, the graph of the change in the total power reflection coefficient with the intensity of the magnetic field was calculated when the linearly polarized electromagnetic wave was incident on the magnetized plasma surface. The best magnetic field strengths of 0.04, 0.07, 0.14, and 0.18 T on the minimum electromagnetic wave reflection power correspond to electromagnetic wave frequencies of 8, 16, 24, and 32 GHz, respectively.

The permeability of plasma can still be regarded as equal to that of the vacuum. Common aerospace materials are used with aluminum alloy, magnesium alloy, alloy steel and composite materials. In Simulation 1 magnetic permeability $\mu_1 = 40\mu_0$, $a = 4$, and $b = 4$; in Simulation 2, permeability $\mu_1 = 20\mu_0$, $a = 1$, and $b = 4$. The calculations of the plasma spherical magnetic field around the object distribution are presented in Fig. 4.
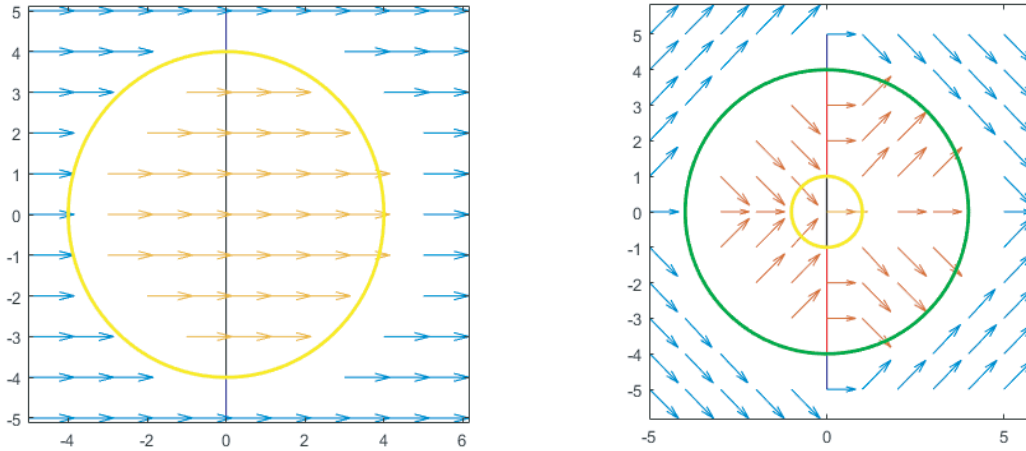
Simulation 1: Magnetic field distribution when $\mu_2/\mu_1 = 0.025$, $a/b = 4/4$ Simulation 2: Magnetic field distribution when $\mu_2/\mu_1 = 0.05$, $a/b = 1/4$

Figure 4. Magnetic distribution map of each region in space of Simulations 1 and 2.

We can obtain the magnetic field distribution of Simulations 1 and 2 through calculation and verification. When μ_2/μ_1 is high and a/b is low, the ratio of the magnetic field strength $H_3(r < a)$ to the magnetic field strength $H_0(r > b)$ is low. When μ_2/μ_1 is low and a/b is high, the ratio of the magnetic field strength $H_3(r < a)$ to the magnetic field strength $H_0(r > b)$ is high.

4. CONCLUSIONS

In this study, we use Laplacian equations in spherical coordinates and consider the ratio of the inner and outer radii of spherical shell plasma, and the size and permeability ratio of the plasma-wrapped object to perform modeling calculations. The magnetic field distribution of each region in spherical space is obtained and further deduced as follows.

When the scalar magnetic field of the external uniform magnetic field is H_0, the magnetic charge of the plasma spherical shell is equivalent to a magnetic dipole on the outside of the magnetic shell.

The magnetic field in the plasma spherical shell is a superposition of a uniform field with a magnetic dipole field [17]. The uniform field is composed of an external uniform field and a uniform field generated by the magnetic charge on the outer surface of the ball. The magnetic dipole field is generated by the magnetic charge on the inner surface of the shell.

When μ_2/μ_1 is high and a/b is low, the ratio of the magnetic field strength H_3 (region $r < a$) to the magnetic field strength H_0 (region $r > b$) is low, and vice versa. When the magnetic permeability of the inner object is small and the spherical shell is thick, the produced plasma sheath is thick, and the external magnetic field in the inner space of the spherical shell is weak. Consequently, the "black barrier" phenomenon will exhibit good shielding effect and high possibility.

REFERENCES

1. Chen, F. F., *Introduction to Plasma Physics*, Plenum Press, New York and London, 1974.
2. Vidmar, R. J., "On the use of atmospheric pressure plasmas as electromagnetic reflectors and absorbers," *IEEE Transactions on Plasma Science*, Vol. 18, No. 4, 733–741, 1990.
3. Laroussi, M. and J. R. Roth, "Numerical calculation of the reflection, absorption, and transmission of microwaves by a nonuniform plasma slab," *IEEE Transactions on Plasma Science*, Vol. 21, No. 4, 366–372, 1993.
4. Mitchell, F. H., "Communication-system blackout during reentry of large vehicles," *Proceedings of the IEEE*, Vol. 55, No. 5, 619–626, 1967.
5. Rybak, J. P. and R. J. Churchill, "Progress in reentry communications," *IEEE Transactions on Aerospace & Electronic Systems*, Vol. 7, No. 5, 879–894, 1971.
6. Liu, J. F., X. L. Xi, and Y. Liu, "A solution to the propagation of electromagnetic wave in plasma sheath using FDTD method," *International Symposium on Antennas*, 442–445, 2008.
7. Kim, M., M. Keidar, and I. D. Boyd, "Electrostatic manipulation of a hypersonic plasma layer: Images of the two-dimensional sheath," *IEEE Transactions on Plasma Science*, Vol. 36, No. 4, 1198–1199, 2008.
8. Liu, J. F., X. L. Xi, G. B. Wan, and L. L. Wang, "Simulation of electromagnetic wave propagation through plasma sheath using the moving-window finite-difference time-domain method," *IEEE Transactions on Plasma Science*, Vol. 39, No. 3, 852–855, 2011.
9. Hodara, H., "The use of magnetic fields in the elimination of the re-entry radio blackout," *Proceedings of the IRE*, Vol. 49, No. 12, 1825–1830, 1961.
10. Russo, F. P. and J. K. Hughs, "Measurments of the effects of static magnetic fields on vhf transmission in ionized flow fields," *NASA: Langley Research Center*, 1964.
11. Russo, F. P., "Electromagnetic wave/magnetoactive plasma sheath interaction for hypersonic vehicle telemetry black out analysis," *34th AIAA Plasmadynamics and Lasers Conference*, Orlando, USA, Jun. 23–26, 2003.

12. Keidar, M., M. Kim, and I. D. Boyd, "Electromagnetic reduction of plasma density during atmospheric reentry and hypersonic flights," *Journal of Spacecraft and Rockets*, Vol. 45, No. 3, 445–453, 2008.

13. Kim, M., M. Keidar, and I. D. Boyd, "Two-dimensional modal of an electromagnetic layer for the mitigation of communication blackout," *47th AIAA Aerospace Sciences Meeting Including the New Horizons Forum and Aerospace Exposition*, 092407, Orlando, Florida, 2009.

14. Tai, Y.-C. and S.-J. Fang, *Electromagnetic Field and Electromagnetic Wave*, 184, Dalian Maritime University Press, 2003 (in Chinese).

15. Zhang, X.-H., *Manufacturing Technology and Practice*, Vol. 22, Beihang University Press, 2011 (in Chinese).

16. Yang, J., L.-M. Zhu, W.-Y. Su, and G.-W. Mao, "Study on calculation of power reflection coefficient of electromagnetic wave on magnetized plasma surface," *Acta Physica Sinica*, Vol. 54, No. 7, 3236–3240, 2005.

17. Guan, J. and H. Zheng, *Electrodynamics*, China University of Petroleum Press, 2015 (in Chinese).